Nuclear Instruments and Methods in Physics Research A293 (1990) 537–544
North-Holland

COMPUTER SIMULATION OF ELECTRON AVALANCHES IN ARGON–METHANE FILLED WIRE CHAMBERS

Jan GROH, Eduard SCHENUIT and Hartwig SPITZER

II Institut für Experimentalphysik, Universität Hamburg, Luruper Chaussee 149, 2000 Hamburg 50, FRG

Received 14 March 1990

A three-dimensional computer simulation of electron avalanches in wire chambers was carried out. Coulomb interactions due to the space charge of the avalanches were taken into consideration. Two gases, Ar/CH_4 (90/10) and Ar/CH_4 (50/50), have been investigated, and studies on the influence of space charges on the avalanche development were performed. Also a brief comparison of two anode diameters, 20 μm and 50 μm, respectively, is presented. A clear radial structure of the gas amplification process is observed. The main amplification takes place within ≈100 μm from the anode, but several partial avalanches can belong to the same primary electron. The arrival times of partial avalanches originating from the same initial electron can deviate by several ns and spatial distances of several hundred μm along the anode have been observed between the partial avalanches. Their FWHM in azimuthal spread is of the order of 45°, the FWHM along the anode wire amounts to ≈25 μm, although the two gas mixtures behave differently. The simulation of space charges in the vicinity of the anode wire supports the assumption that electron–ion recombination and photon emission and absorption are of major importance for shielding effects. The obtained results are in good agreement with earlier simulations and experimental investigations.

1. Introduction

One of the least understood physical processes in wire chambers is the gas amplification. The microscopic dimensions as well as the fast development of the electron avalanches around the anode wires prevent measurements of the detailed structure of the charge multiplication process. Nevertheless some important insights into the global properties have been gained throughout the last decades. In 1955, Raether [1] used cloud chambers to take photographs of streamer discharges. Meanwhile, several experiments have been carried out to determine the longitudinal and azimuthal profile of electron avalanches in proportional chambers (see e.g. refs. [2–6]). They made use of the onset of shielding effects in the amplification of electrons from primary tracks inclined against the anode wire (Schultz, Kröger) and the induced current in strip cathodes surrounding the anode wire (Fischer et al.), respectively. In argon–propane 95–5%, operating with a gas gain of 5×10^4, Kröger found a full width of the avalanche along the anode of ≈50 μm, the wire having a diameter of 50 μm. Using a somewhat higher gas gain, Schultz found a full width of 65 μm. For the azimuthal spread Fischer et al. found a full width at half maximum (FWHM) value of $(80 \pm 10)°$ for a gas gain of 10^4 in argon–methane 90–10% with an anode diameter of 25.4 μm. Actually they present data from a whole range of amplification factors and gas mixtures but these will not be discussed in this work. All experiments used particle beams which led to a significant number of primary electrons. Thus the properties of avalanches deriving from single primary electrons had to be estimated from the global measurements.

Due to the experimental difficulties, semitheoretical approaches and computer simulations early found attention. Several parametrizations of experimental data on the first Townsend coefficient α/p (p is the pressure) and the gas amplification factor M have been suggested since the 1940's as functions of the chosen gas and the reduced electric field E/p [7–13]. Yet a conclusive physical derivation of the formulas could not be demonstrated.

On the other hand, early Monte Carlo simulations of electron avalanches in homogeneous electric fields showed that the first Townsend coefficient usually will not attend its equilibrium value if there is a significant gradient of the field. Folkard and Haydon [14] found that in homogeneous fields particles have to pass through a potential difference of about 70 V to reach the final value of α in hydrogen. Experimental checks confirmed this result. Thomas and Thomas [15] demonstrated that the mean energy of an electron ensemble $\bar{\epsilon}$ is not reached before the particles have passed a potential difference of $\Delta V \geq 5\bar{\epsilon}/e$. They showed that the ergodic hypothesis is in general not applicable to electron avalanches. Sato and Tagashira [16] simulated electrons in nitrogen which were exposed to a gradient of the electric field of 10^6 V/cm^2. Although they did not observe significant deviations of $\bar{\epsilon}$ or the drift velocity

v_d from their equilibrium values, α deviated up to several orders in magnitude from its equilibrium value in a homogeneous field.

These results favour Monte Carlo techniques, i.e. tracing of the particles on microscopic scale, for the simulation of electron avalanches in wire chambers. Thomas and Thomas carried out an early investigation of avalanches in homogeneous electric fields at the end of the sixties [15]. They traced each single electron through all its collisions until it reached the anode. Secondary electrons created by ionization were recorded together with the coordinates of their production and velocity. Like the initial electron they were followed successively until all the particles had been collected at the anode plane. The same technique was used by several other investigations (e.g. refs. [14,17,18]) which excellently reproduced macroscopic parameters of electron motion in gases, as e.g. the drift velocity and the diffusion coefficients.

Investigations of nonhomogeneous electric fields were carried out by Sato and Tagashira [16], Kunhardt and Tzeng [19], and Matoba et al. [20]. Kunhardt and Tzeng for the first time incorporated the Coulomb interaction of the charges inside an avalanche exposed to a homogeneous outer electric field. This was possible because they traced the electrons parallel in time. Matoba et al. were the first to perform a three-dimensional Monte Carlo simulation in cylindrical geometry but moved the electrons one after the other each through its whole path. Thus Coulomb interactions between charged particles, i.e. shielding effects, could not be taken into consideration.

In this work we present further results from a computer simulation of electron avalanches in argon–methane filled wire chambers which for the first time include the outer cylindrical field geometry as well as the Coulomb interaction between the charges inside the avalanches. Our investigation aimed at the time and spatial structure of electron avalanches and the influence of shielding processes on their development. For the first time, results are based on a statistically significant number of avalanches.

First results and some outlines of the computer program ELAVA have been published elsewhere [21,22]. A detailed discussion of ELAVA and its development can be found in ref. [23].

2. Method

Electron avalanches were simulated in a mixed molecular dynamics and Monte Carlo technique. The electrons were traced in six-dimensional phase space and assumed to be subject to the cylindrically symmetric field of the anode–cathode configuration as well as the Coulomb interaction with the ionic and electronic charges inside the avalanche. A fast and precise algorithm, the so-called *leap-frog algorithm* (compare e.g. ref. [24]), was used to move the particles. Collisions with gas molecules were simulated on the basis of momentum-transfer cross sections which were extracted from literature. Elastic, excitation, and ionization cross sections were compiled for argon [25–29] and methane [30–36]. Energy but not momentum was conserved in the collisions. Gas molecules and ions were assumed to be of infinite mass and fixed in space. This reflects the much lower mobility of ions as compared to electrons. The motion of ions takes place in the ns to μs region while the electrons move on the ps scale. Scattering was assumed to be isotropic. No secondary processes as electron–ion recombination and photon emission or absorption were taken into account for this simulation.

The incorporation of *shielding effects*, i.e. effects due to the Coulomb interaction between avalanche particles, made it necessary to move all electrons parallel in time. To achieve this, a mean time of free flight was calculated from the mean energy per electron of the ensemble and the two sets of cross sections. Occurrences of scatterings then were calculated with the help of a null collision technique (compare e.g. refs. [37–39]). Thus, the energy spectrum of the electrons and the energy dependence of the collision cross sections were taken into account at any given time.

The large number of charged particles in the avalanches – up to 10^5 in our simulation – prevented a direct calculation of the Coulomb interaction. Inspired by works of Kunhardt and Tzeng [19] and by methods known from plasma physics [24] a technique was developed which approximated the distribution of charges with the help of a three-dimensional mathematical lattice. A summary of the technique can be found in ref. [22], while a fully detailed description is included in ref. [23]. Therefore only an outline will be given here: According to a weighting algorithm, the charges of electrons and ions are spread on the mathematical lattice which extends in r (radial), ϕ (azimuthal), and z (along the anode) direction. Coulomb interaction of charges at the lattice points is then calculated with the help of tabulated distances between the points. This procedure drastically increases the speed of the calculation. The field strength at the position of the electrons is interpolated from the lattice according to the inverse weighting algorithm used for the spreading of the charges. To further increase the speed of computation two separate lattices were used. One for charges in motion (free electrons) and one for charges fixed in space (ions and captured electrons), which were superposed for the calculation of the electric field. The lattice of free electron charges was updated when the total number of electrons had changed by 3%. This corresponds to a time span of about 2 ps.

Table 1
Parameter sets for chamber definition

Parameter set:	no. 1	no. 2	no. 3
Anode radius r_a [μm]	10	10	25
Cathode radius r_c [mm]	5	5	5
Anode voltage U_a [V]	1300	1500	1600
Gas: argon [%]	90	50	90
methane [%]	10	50	10
Temperature T [K]	300	300	300
Pressure p [hPa]	1013	1013	1013
Mean gas gain	≈10000	≈10000	≈10000

The chamber properties were determined by anode radius, cathode radius, anode voltage, temperature, pressure, and gas mixture. But only the gas mixture, the anode voltage, and the anode radius were varied in this investigation. The different parameter sets are listed in table 1.

3. Results

Because of the computer time consumption (up to 75 min of IBM-3084 equivalent cpu time per avalanche) the investigation had to focus on a few topics of major interest. We concentrated on the spatial dimensions of the avalanches in two gases, argon–methane 90–10% and Ar–CH_4 50–50%, and on the influence of shielding effects on the gas amplification. A less detailed investigation was carried out for Ar/CH_4 90/10 with an anode radius of 25 μm (compare table 1).

Unshielded avalanches were simulated with all three parameter sets, but statistically significant amounts of data were accumulated only with sets 1 and 2. The single primary electrons were released at 1000 μm from the anode wire. Results were extracted from ensembles of 100 avalanches for each gas mixture and pre-established space charge. Figs. 1 and 2 show typical avalanches in Ar/CH_4 90/10 and Ar/CH_4 50/50,

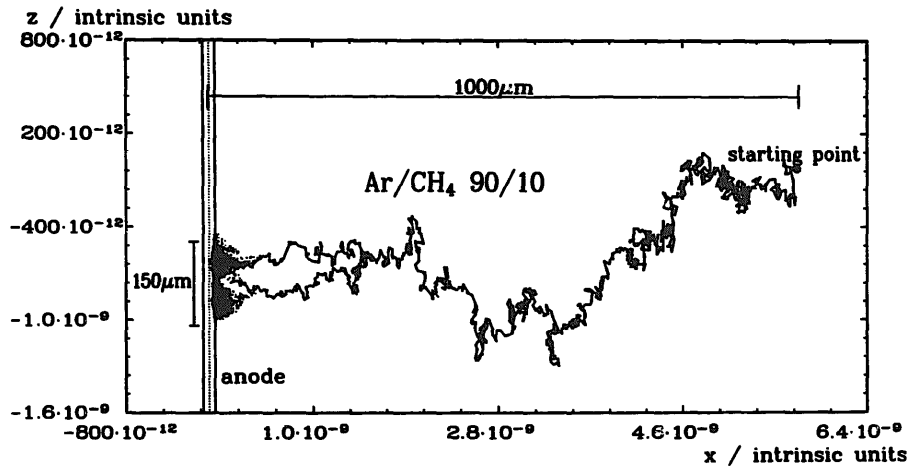

Fig. 1. Complete avalanche of a single primary electron in Ar/CH_4 90/10.

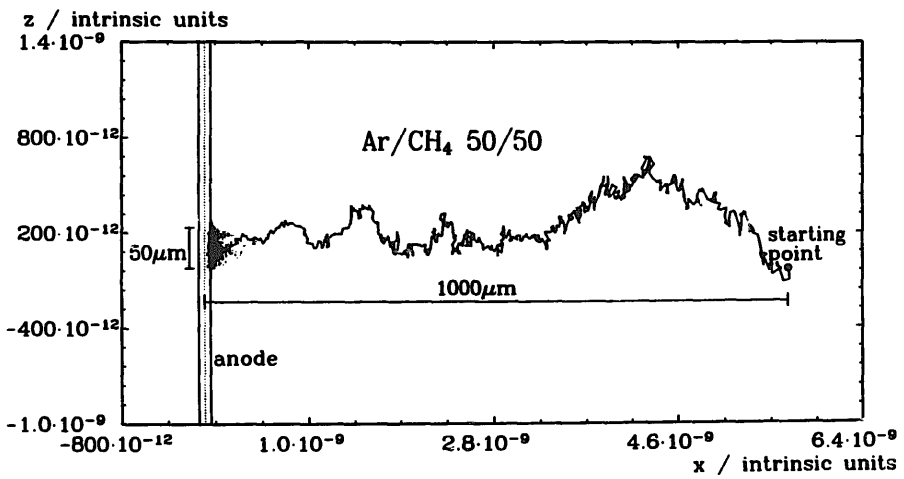

Fig. 2. Complete avalanche of a single primary electron in Ar/CH_4 50/50.

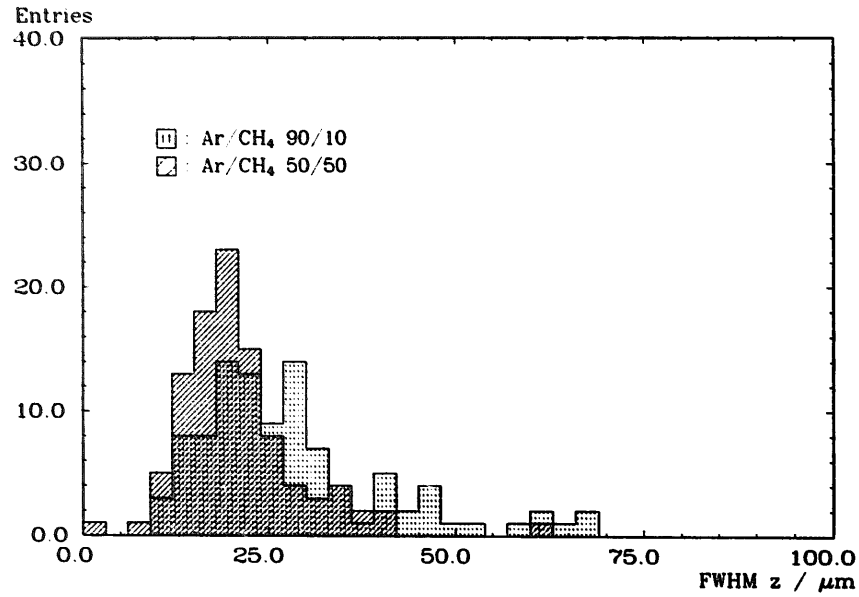

Fig. 3. Histograms of FWHM of z distribution in Ar/CH_4 90/10 and Ar/CH_4 50/50, respectively.

respectively (to save computer time some special intrinsic units have been used for the coordinates which are of no importance here). The plots present a superposition of recordings of electron positions in the avalanche taken every few ps. The path of the initial and the first secondary electron in fig. 1 is indicated by the solid lines. Only a few percent of the scatterings have been recorded in these plots. The different behaviour of the two gases is obvious. In Ar/CH_4 90/10 the electron's path is curled, first ionizations occur at several hundred μm from the anode. Several partial avalanches lead to a spread in z up to some hundred μm along the anode wire and to differences in the arrival times between the partial avalanches in the order of ns. In Ar/CH_4 50/50 the electron's path is much straighter, ionizations occur only inside a radius of roughly 100 μm from the anode, and no clearly distinguished partial avalanches are observed. The difference between the gas mixtures can also be seen from figs. 3 and 4 where the FWHM of the z and azimuthal spread of partial avalanches are compared for the two gases, respectively. These results were obtained by releasing single electrons at a distance of

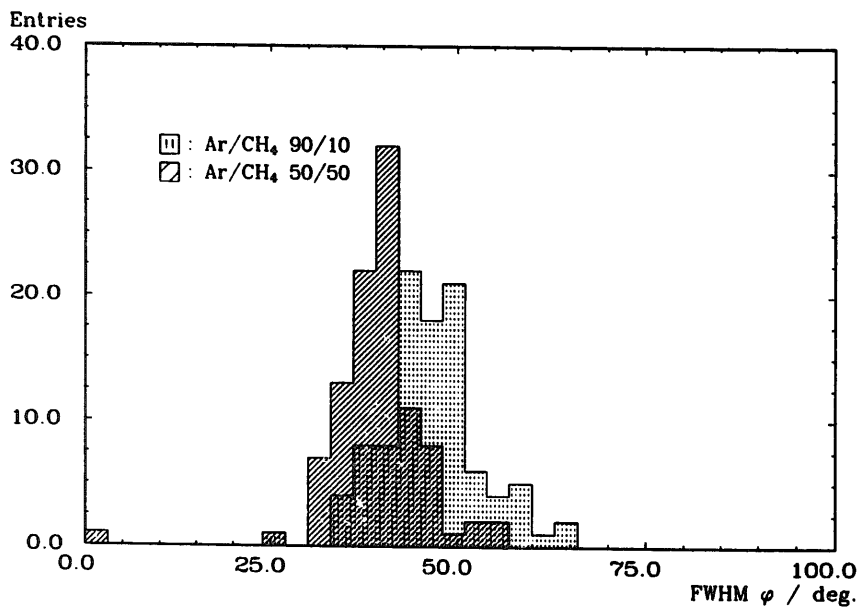

Fig. 4. Histograms of FWHM of azimuthal distribution in Ar/CH_4 90/10 and Ar/CH_4 50/50, respectively.

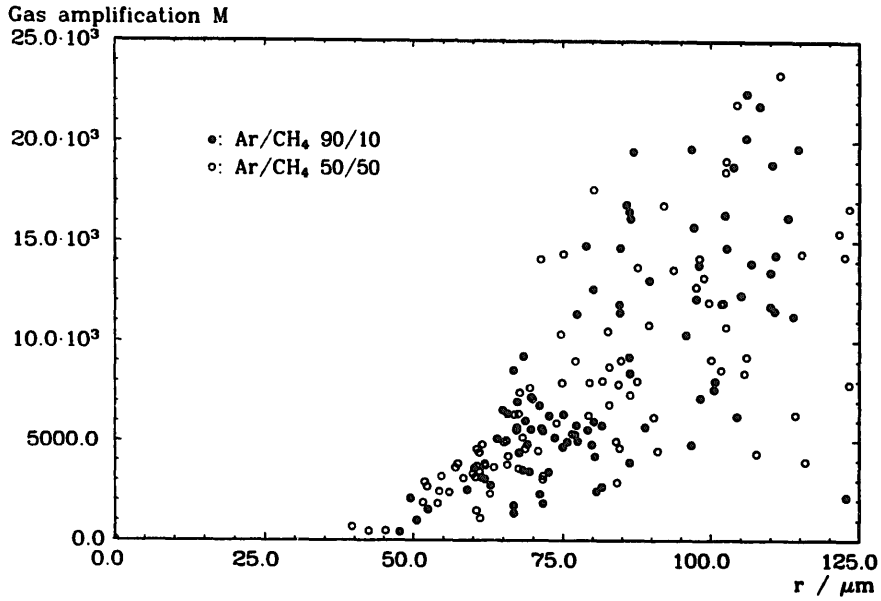

Fig. 5. Correlation of radius of first ionization, r, and gas amplification M in Ar/CH_4 90/10 and Ar/CH_4 50/50, respectively.

≈ 125 μm from the anode and adjusting the gas amplification to a mean value of approximately 10^4 in both cases. In z as well as in the azimuthal spread Ar/CH_4 90/10 shows a larger mean value and bigger fluctuations in the FWHM distribution: ≈ 25 μm versus ≈ 20 μm, and ≈ 47° versus ≈ 40°, respectively. The radial structure of the partial avalanches shows no significant difference, as indicated by fig. 5. Here the gas amplification in the partial avalanches is plotted versus the radius r of the production of the first secondary electron. Nevertheless, the completion of a partial avalanche in Ar/CH_4 90/10 takes ≈ 1100 ps compared to ≈ 800 ps in Ar/CH_4 50/50. This difference is mainly due to the different drift velocity in the two gases since the main amplification process, which takes place close to the wire (a few μm), lasts approximately the same 400 to 600 ps in both gases.

The *simulation of shielding effects* due to the spatial and time overlap of two partial avalanches made use of the mathematical lattices which had been invented for

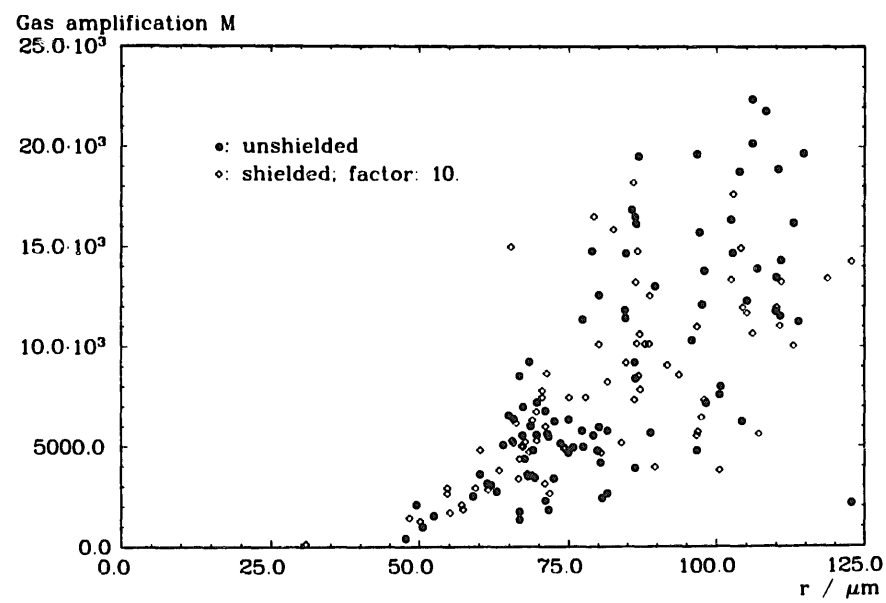

Fig. 6. Correlation of radius of first ionization, r, and gas amplification M in Ar/CH_4 90/10 without shielding and with shielding factor 10.

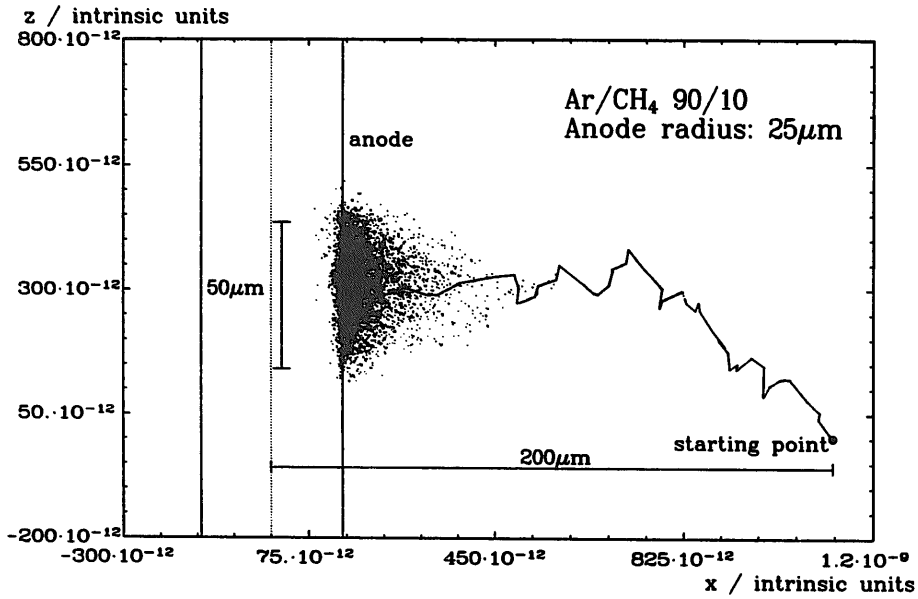

Fig. 7. Partial avalanche in Ar/CH_4 90/10, anode radius 25 μm.

the calculation of the Coulomb interaction. The final condition of the fixed charges' lattice (ions and electrons on the wire) of a typical partial avalanche (gas gain 11 500) was taken as initial condition of the lattice for the simulation of follow-on avalanches (*shielded partial avalanches*). This assumption of course oversimplifies the processes in the vicinity of the anode wire. But since the mobility of the ions is much smaller than that of the electrons, and in real chambers large numbers of partial avalanches develop in just a few ns with high spatial density, the method should give at least an impression of the effects of shielding due to space charges around the sense wire.

An ensemble of 100 shielded partial avalanches was simulated, but no significant difference in any of the recorded parameters such as z- and ϕ-distribution, gas gain, and radial structure was observed. The investigation was repeated with the initial lattice charges enlarged by a factor of 10, but again no significant change in z, ϕ, and gas gain was observed. Yet, the radial structure of the avalanches showed some new properties. While the correlation between gas gain and radius

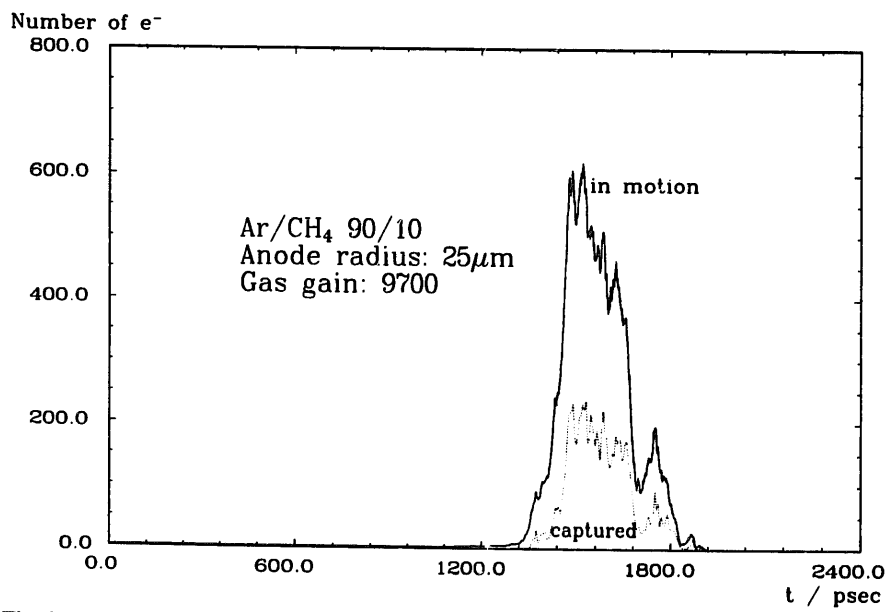

Fig. 8. Time development of a partial avalanche in Ar/CH_4 90/10, anode radius 25 μm.

of first ionization was not affected, compare in fig. 6, the centre of charge of the electron lattice moved farther away from the anode surface. This effect was further emphasized, when the scaling factor was increased to 20, 50, and 100. The space charge then led to radial oscillations of the electrons in a region between 2 μm and 5 μm over the anode surface. This oscillation is due to the strong electric field between the electron charges on the anode surface and the ion charges in space combined with the electric field of the wire. The assumption of the electrons still being fixed on the wire surface is crude but necessary as long as the ions are regarded as fixed in space.

Only few electrons pass the area of low electric field between the wire and the bulk of the positive ion charges. Thus the time needed for the development of the avalanche is increased significantly. Although the physical model included in ELAVA certainly is overstressed under these conditions, the simulations indicate that the process of shielding is more complicated than a mere decrease of the gas amplification due to a weaker electric field in the vicinity of the anode. At high charge densities, recombination of electrons and atoms/ions and photon emission and absorption become of greater importance. These effects have not been incorporated in ELAVA.

To investigate the *influence of the sense wire's diameter* on the avalanche development, a few avalanches were simulated with parameter set 3. Figs. 7 and 8 show the spatial and time development of a typical partial avalanche, respectively. In fig. 8 the solid line gives the number of electrons drifting to the anode as a function of time t. The dotted line represents the number of electrons captured by the anode wire in each interval of 5 ps around t as a function of t. As expected from the geometry of the electric field the amplification region reaches farther out from the anode, the angular spread is smaller than and the z spread identical to the simulations with set 1. This behaviour is expected under the assumption that the spatial (and time) dimensions of the avalanches are determined solely by diffusion. This assumption is supported by our studies of shielding effects, presented above, since no deviations in the space and time development could be observed between shielded and unshielded avalanches. As expected, fluctuations in the gas gain were bigger than with parameter set 1. Due to the smaller gradient of the electric field the onset of ionization is smeared out over a wider radial range.

4. Discussion

The results of our investigation are in good agreement with the earlier computer simulation of Matoba et al. [20] and experiments of refs. [2,3,6]. For the comparison of the two simulations it has to be taken into account that different gases, anode voltages, and anode diameters were used. Matoba et al. do not present the statistics on which they based their analysis. They give a FWHM of the avalanche's angular spread of 30–40° for an anode diameter of 25 μm (cathode radius 5 mm) in pure argon and in argon with admixtures of CO_2. This is in reasonable agreement with the mean FWHM of the azimuthal spread of ≈ 40° and ≈ 47° which we found in Ar/CH_4 50/50 and 90/10, respectively. Our investigation supports their interpretation of the deviation of a factor of two to experimental data (from ref. [6]) given by Matoba et al. Studies on full avalanches, which were initiated by electrons released 1000 μm from the anode, revealed fluctuations of the order ±20° in the centre of charge between partial avalanches. Taking into consideration the large number of primary electrons in experimental investigations, a measured FWHM in the azimuthal spread is expected to be some 20 to 40° bigger than for partial avalanches. Therefore our results are in good agreement with the angular spread of some 80° given by Fischer et al. [6].

Since Matoba et al. present only data obtained with electrons released 100 μm from the anode, no hints on the particular radial and time structure of full avalanches can be found in their work. Therefore their results have to be compared to the *partial avalanches* of this investigation.

The occurrence of several partial avalanches initiated by a single primary electron and its consequences for the interpretation of chamber data was first pointed out in an earlier work of the authors [22]. The comparison of Ar/CH_4 90/10 and 50/50 proves that the particular structure of the avalanches strongly depends on the chosen gas. It would be interesting to discuss differences between the operational properties of gases on this level.

Fig. 7 of the work of Matoba et al. suggests a value comparable to the mean FWHM of ≈ 20 μm and ≈ 25 μm for the z spread which we found in Ar/CH_4 50/50 and 90/10, respectively. Kröger [3] and Schultz [2] derived full widths in z of 50 μm at a gas gain of 5.1×10^4, and 65 μm at a higher gain, respectively. As a criterion for the avalanche extension they used the onset of shielding effects. In fact, this method is not applicable to study the size of avalanches but only the critical charge density, since it cannot resolve whether the charges originate from a single primary electron or a whole bunch. Nevertheless, the charge densities present a limit for the onset of shielding effects. A number of 5×10^4 electrons per 50 μm matches roughly with the factor-10 shielding investigated in this work. It was already stated above that the physical model implemented in ELAVA reaches its limits at this value of the space charge, since recombination and photon emission/absorption are no longer negligible. The assump-

tion of a fundamental change in the gas amplification process at charge densities of $\approx 5 \times 10^4$ is therefore supported by this work.

As mentioned above, results from the simulation of avalanches with an enlarged anode diameter fit into this picture of the gas amplification process and agree with usual expectations.

It should be emphasized that uncertainties and oversimplifications in the description of the scattering processes naturally influence the results of this investigation. Dimensions and features of avalanches presented in this work therefore should be understood as qualitative, but not as precise calculations. A more detailed discussion of this problem can be found in ref. [23].

5. Summary and conclusion

Results from a computer simulation of electron avalanches in Ar/CH_4 90/10 and Ar/CH_4 50/50 have been presented, respectively. A clear radial structure was found in the gas amplification process, which depends on the gas mixture and the anode diameter. The FWHM in z and the azimuthal spread of partial avalanches are of the order of 25 μm and 45°, respectively, which is in good agreement with earlier simulations and experimental studies. The investigation of shielding effects led to the conclusion that a model of the involved processes has to incorporate electron–ion recombination as well as photon emission and absorption by the chamber gas.

Acknowledgement

We would like to thank H. Nierobisch from III Physikalisches Institut der RWTH Aachen for many helpful discussions.

References

[1] H. Raether, Z. Angew. Phys. 7 (1955) 50.
[2] G. Schultz, Etude d'un Detecteur de Particules à tres haute Precision Spatiale (Chambre à Drift), thesis (Strasbourg, 1976).
[3] B. Kröger, Driftzeit- und Impulshöhenmessung mit quadratischen Proportionaldriftrohren, DESY internal rep. F1-77/03 (1977).
[4] J. Fischer et al., IEEE Trans. Nucl. Sci. NS-25 (1978) 794.
[5] J. Fischer et al., Nucl. Instr. and Meth. 151 (1978) 451.
[6] J. Fischer et al., IEEE Trans. Nucl. Sci. NS-26 (1979) 160.
[7] M.E. Rose and S.S. Korff, Phys. Rev. 59 (1941) 850.
[8] L.G. Khristov, Dok. Bulg. Akad. Nauk. 10 (1947) 453.
[9] W. Diethorn, US Atomic Energy Commission rep. NYO-6628 (1956).
[10] A. Williams and R.I. Sara, Int. J. Appl. Radiat. and Isot. 13 (1962) 229.
[11] A. Zastawny, J. Sci. Instrum. 44 (1967) 395.
[12] M.W. Charles, J. Phys. E5 (1972) 95.
[13] T.Z. Kowalski, Nucl. Instr. and Meth. A234 (1985) 521.
[14] M.A. Folkard and S.C. Haydon, Aust. J. Phys. 23 (1970) 847.
[15] R.W.L. Thomas and W.R.L. Thomas, J. Phys. B2 (1969) 562.
[16] N. Sato and H. Tagashira, J. Phys. D18 (1985) 2451.
[17] H.T. Saelee and J. Lucas, J. Phys. D10 (1977) 343.
[18] H.N. Kücükarpaci and J. Lucas, J. Phys. D14 (1981) 2001.
[19] E.E. Kunhardt and Y. Tzeng, J. Comput. Phys. 67 (1986) 279.
[20] M. Matoba et al., IEEE Trans. Nucl. Sci. NS-32 (1985) 541.
[21] J. Groh – ELAVA, Computer Program for the Simulation of Electron Avalanches in Electric Fields (Hamburg, 1988) unpublished.
[22] J. Groh, E. Schenuit and H. Spitzer, Nucl. Instr. and Meth. A283 (1989) 730.
[23] J. Groh, Diploma Thesis, DESY internal rep. FH1T-89-03 (Hamburg, 1989).
[24] C.K. Birdsall and A.B. Langdon, Plasma Physics via Computer Simulation (McGraw–Hill, New York, 1983).
[25] H.B. Milloy et al., Aust. J. Phys. 30 (1977) 61.
[26] S.K. Srivastava et al., Phys. Rev. A23 (1981) 2156.
[27] A. Chutjian and D.C. Cartwright, Phys. Rev. A23 (1981) 2178.
[28] J. Bretagne et al., J. Phys. D19 (1986) 761.
[29] R.C. Wetzel et al., Phys. Rev. A35 (1987) 559.
[30] B. Schmidt, Dissertation, Universität Heidelberg (1986).
[31] H. Tanaka et al., J. Phys. B15 (1982) 3305.
[32] A. Jain and D.G. Thompson, J. Phys. B16 (1983) 3077.
[33] K. Rohr, J. Phys. B13 (1980) 4897.
[34] L. Vušković and S. Trajmar, J. Chem. Phys. 78 (1983) 4947.
[35] D. Mathur, J. Phys. B13 (1980) 4703.
[36] O.J. Orient and S.K. Srivastava, J. Phys. B20 (1987) 3923.
[37] J. von Neumann, NBS Appl. Math. 12 (1951) 36.
[38] H.R. Skullerud, J. Phys. D1 (1968) 416.
[39] S.L. Lin and J.N. Bardsley, Comput. Phys. Commun. 15 (1978) 161.